

On the Electrodynamics of Charge Density Waves: Classical vs. Quantum Formulations

A. Beckwith

Physics department
Chongqing University
College of Physics, Chongqing University Huxi Campus
No. 55 Daxuechen Nanlu, Shapingba District, Chongqing 401331
which is in Chinese:重庆市沙坪坝区大学城南路55号重庆大学虎溪校区
People's Republic of China
Rwill9955b@gmail.com

Abstract

We show that the classical random pinning model, if simulated numerically using a phase evolution scheme pioneered by Littlewood, gives dispersion relationships that are inconsistent with experimental values near threshold. These results suggest the need for a revision of contemporary classical models of charge density wave transport phenomena. Classical phase evolution equations have the same form as driven harmonic oscillators. We provide a different formulation of charge density transport using a tunneling Hamiltonian, motivated by Sidney Coleman's false vacuum hypothesis, to model soliton anti-soliton pair transport through a pinning gap. We thereby derive an analytical expression for charge density wave transport that agrees with experimental data both above and below the threshold field.

Introduction

In 1986, Littlewood [1] presented an innovative scheme to model charge density waves which incorporates the classical phase pinning model of Fukuyama, Lee, and Rice [2,3] for the interaction of impurities on a one dimensional lattice. We note that this numerical scheme employs a discretized Sine- Gordon equation [4] for the phase evolution along a one-dimensional crystal. With the impurity sites randomly distributed, the interaction potential is written as $V_j (x - R_j) = V\delta(x - R_j)$ for short-range interaction between the phase $\phi(x)$ and impurity site R_j where V is the interaction strength at the impurity sites. The variable R_j (denoting the impurity position) is randomly chosen with $R_{j+1} > R_j$. A first order, overdamped equation for the phase $\phi(x_j) = \phi_j$ is solved on this lattice where $x_j = cR_j$ and c is the impurity concentration. Assuming a correlation length L , $cL^d \gg 1$ for weak pinning where d is the dimensionality of the spatial integration (set equal to 1.0 in our simulation). Conductivity and dielectric values are obtained from the Discrete Fourier Transform DFT of the CDW current $J(t) \propto \left\langle \dot{\phi} \right\rangle(t)$ as a function of the excitation frequency ω .

In the classical model demonstrated next, the CDW current is calculated from the time derivative of the phase averaged over the one-dimensional lattice. In the quantum tunneling section, we derive a formula for the CDW current that agrees with experimental I - E measurements above and below threshold by considering soliton

anti-soliton pair tunneling through a pinning gap. Furthermore, the quantum model eliminates singular behavior evident in the classical model near threshold.

[insert figure 1 about here]

II. Classical Random Pinning Model: Numerical Simulation

We took care to avoid positioning impurity sites too close to the origin which could result in spurious numerical values for the phase time derivative leading to non physical results for physical quantities such as conductivity even when the applied E field is $< E_{th}$. A stable average phase is observed in Figure 1 for $E < E_{th}$ whereas a continuously increasing phase value is observed if $E > E_{th}$. Diverging values of the ac conductivity can result above threshold, however.

In equation one the applied field E has both constant dc and oscillatory ac contributions [5]. The term $\Delta^2\phi_i$ represents the CDW phase interaction between adjacent impurity sites randomly located at $X_i = cR_i$ with $R_i > R_{i-1}$.

$$\dot{\phi}_i = \Delta^2\phi_i + \frac{1}{2}E(X_{i+1} - X_i) + V \sin(\theta_i + \phi_i) \quad (1)$$

In this equation the inertial term proportional to $\ddot{\phi}$ is set equal to zero. θ_i represents a randomized force which varies between zero and 2π . The second derivative is discretized on interior lattice sites following [6,7,8]

$$\Delta^2\phi_i = \frac{\phi_{i+1} - \phi_i}{X_{i+1} - X_i} - \frac{\phi_i - \phi_{i-1}}{X_i - X_{i-1}} \quad (2)$$

Periodic boundary conditions are applied by writing the Laplacian as [9]

$$\Delta^2\phi_1 = \frac{\phi_2 - \phi_1}{X_2 - X_1} - \frac{\phi_1 - \phi_N}{X_1 - (X_N - L)}, \quad (3)$$

as well as

$$\Delta^2 \phi_N = \frac{\phi_1 - \phi_N}{X_1 - (X_N - L)} - \frac{\phi_N - \phi_{N-1}}{X_N - X_{N-1}}, \quad (4)$$

where L is the grid length.

III. Electromagnetic Properties Near Threshold

The real part of the ac conductivity is obtained from a DFT of equation (1) according to

$$\text{Re } \sigma(\omega) \propto g_1 \sum_n \left\langle \dot{\phi} \right\rangle_n \cos(\omega t_n) \cdot \Delta t, \quad (5)$$

while the imaginary part is given by

$$\text{Im } \sigma(\omega) \propto g_1 \sum_n \left\langle \dot{\phi} \right\rangle_n \sin(\omega t_n) \cdot \Delta t. \quad (6)$$

We note that $\left\langle \dot{\phi} \right\rangle(t)$ is calculated via 2nd order Runge Kutta procedure. To avoid first order round off and truncation, the DFT is performed inside the same Runge-Kutta subroutine. Here, n is the discrete time index where $t_n = n\Delta t$.

Including in both DC and AC contributions to an electric field, we set

$$E = E_{\text{dc}} + E_{\text{ac}} \sin(\omega \tau) \quad (7)$$

When these electric field values are put into both Equation 1 and either equations 5 and 6 of the conductivity equations, we get striking conductivity graphs for both real

[insert figure 2 about here]

and imaginary parts with the following qualitative features. When the electric field applied to a sample is defined by equation 7, and we look at the conductivity, we have that there is a critical value ω_c for frequency in which the imaginary conductivity goes through an inflection point and decreases, provided that we are setting $E = E_{dc}$ in equations 5 and 6 above which can be seen in figure 2. Here, ω_c is this critical value for frequency, which presupposes that the modulus of the applied electric field is below a threshold value, E_{th} . We should note that ω_c varies for different materials. Furthermore, we also have dielectric plots which are plotted against increasing frequency according to:

$$\text{Re } \varepsilon(\omega) = 4\pi \left(\frac{\text{Im } \sigma(\omega)}{\omega} \right) \quad (8)$$

as well as

$$\text{Im } \varepsilon(\omega) = 4\pi \left(\frac{\text{Re } \sigma(\omega)}{\omega} \right) \quad (9)$$

We find that if we re-scale dielectric measurements versus an applied electric field by resetting $\varepsilon/\varepsilon_{initial}$ in place of just ε versus E field (applied to an experimental sample) that as the frequency ω gets much smaller than ω_c we observe increasingly non linear dielectric behavior as the E field approaches E_{th} . We observe an almost linear line plot dependence of dielectric values on the E field if $\omega \approx \omega_c$ almost up to where the applied electric field has a magnitude $E \approx E_{th}$. This is striking, because when we have an applied electric field with a magnitude at or just above E_{th} we observe the dielectric value with singular behavior. This is shown in the almost flat graph of when the frequency divided by ω_c is either 0.75 or one in figure 3.

[insert figure 3 about here]

On the other hand, figure 4 has wildly divergent plots as frequency drops to $0.3 \omega_c$. Figure 4 compares several dielectric plot results. Even when an electric field

[insert figure 4 about here]

being applied to a quasi one dimensional material (e.g. NbSe₃) has a modulus value below a threshold field value, the results shown in the following dielectric plots do not have experimental verification.

What is not shown in these figures is the singularity blow up in dielectric response as the applied electric field reaches the so called threshold value. Interestingly enough, Figures 3, and 4 say that the non linearity in the response actually increases as $\frac{\omega}{\omega_c} \rightarrow 1$. By this, as $\omega \rightarrow \omega_c$ we observe that there is a flattening

of the dielectric response of the material so long as $E < E_{th}$. The abrupt transition to an ‘infinite’ dielectric value actually becomes more pronounced as $\frac{\omega}{\omega_c} \rightarrow 1$. In

addition, we have in Figure 2 a demonstration of what we can simulate for conductivity when simulating results with applied electric fields that are below a threshold value. Below a threshold electric field value (which is the modulus of the applied electric field to a sample) the agreement with classical results is adequate.

This abruptly changes as one passes the applied electric field value. So why does a classical model of conductivity perform well when an electric field is applied to, say, an NbSe₃ crystal in low temperatures, and then perform so poorly in regions in which we pass a threshold value for the applied electric field to the NbSe₃ sample? An

obvious answer is to consider dissipative effects, or lack thereof, as contributing to unwanted surge in calculated conductivity values when $E \geq E_{th}$ and appearing to signify almost discontinuous behavior in the conductivity and dielectric calculations when $E \approx E_{th}$. This is similar to a damped driven harmonic oscillator giving marked divergent behavior if the amount of energy put into the system exceeds what is dissipated out.

IV Quantum Version of CDW Conductivity

Let us now present the quantum version of the conductivity measurements. To do this, we should consider, as was not done before, what happens to quasi one dimensional metals which are exposed to electric fields above a threshold value, E_T , which also are below the Perils temperature, signifying the onset of CDW. To do this, we shall set a constant electric field above the requisite electric field strength E_T partly because we do not have a corresponding theory for alternating fields. In the appendix, I make reference to a functional form of the current which is proportional to:

$$(T_{IF})_{functional} \Big|_{\Psi(real)} = \frac{-c_1}{2\mu} \int \left(\Psi_{initial}^* \frac{\delta \Psi_{final}}{\delta \phi(x)} - \Psi_{final} \frac{\delta \Psi_{initial}^*}{\delta \phi(x)} \right) \delta(\phi(x) - \phi_0(x)) \delta \phi(x) \quad (10)$$

where the wave functionals mentioned above were thin wall approximations to the soliton-anti soliton pair which was written by having:

$$\Psi_{initial,final} = c_{initial,final} \cdot \exp(-\alpha \cdot \int dx [\phi - \phi_{classical}]_{initial,final}^2) \quad (11)$$

with

$$[\phi - \phi_{classical}]_{initial,final} \approx \left[\frac{1}{L} \cdot \sum_n e^{-ik_n \cdot x_i} \phi(k_n) \right] \quad (12)$$

This $\Psi_{initial,final}$ wavefunctional is very similar to being a Gaussian functional with a given covariance Ω of the sort one can use to represent a ‘Fock’ vacuum space [21], as we mention in appendix A. In addition, we should note that the $\oint \phi$ expression is a way of denoting a functional integral over varying $\phi(x)$ path. Also, the thin wall approximation is used via a Fourier transform of a square pulse we set up via:

$$\phi(k_n) = \sqrt{\frac{2}{\pi}} \cdot \frac{\sin(k_n L/2)}{k_n} \quad (13)$$

The upshot is that we obtained a current calculation which, unlike the Zener tunneling expression we will refer to later has a zero value for direct current applied field values below a given threshold value down to when the applied electric field is zero valued. By way of comparison, we should note that the Zener expression for current becomes negative valued whenever an applied constant electric field is below a threshold value. This shows up in figure seven of this paper.

In addition, our attention will be focused upon the differential conductivity which is :

$$(\sigma_{DC})_d = \frac{d\langle j \rangle}{dE} \quad (14)$$

which has unique properties when $E \rightarrow E_T$. In the classical model as given by Gruner [11] during the 1980s we may write:

$$(\sigma_{DC})_d = \frac{n \cdot e^2}{m^* \cdot \left(1 - \frac{E_T}{E}\right)^{1/2}} \quad (15)$$

The singularity which results when we have an applied field achieve a threshold value is, in this case a consequence of resonance behavior of CDW occurring when the deep damping condition for the evolution of phase ϕ break down , i.e. when $\ddot{\phi} \neq 0$, indicating a situation characterized by rapidly increasing energy to CDW trapped within a potential barrier region. There exists classical models of CDW which avoid this singular behavior by treating the threshold field as a dynamical critical phenomon. Our objection to these models is in the highly arbitrary conditions placed upon the potentials used for the quasi one dimensional lattice, which are in many ways without the innate simplicity given by the overdamped driven oscillator model for phase evolution.

We can note something about the quantum model pertinent to this transport problem if we state that the initially classical treatment of CDW transport has been reformulated in terms of a tunneling Hamiltonian to avoid having to work with hard to visualize and possibly very non intuitive potentials [24]. We started with John Bardeens pioneering work in 1960-61 [16] which was considering transport of single electrons through a barrier with wave functions put into a quasi particle representation. Unlike Bardeen, who incorrectly assumed that a Cooper pair could not penetrate through a potential barrier, we used soliton- anti soliton pairs traversing a pinning gap for representing charge density wave transport, thereby managing to

formulate a tunneling Hamiltonian proportional to current. This derived current is shown later to be very much in sync with experimental measurements.

In addition, we have that we found it most useful to use wave functionals in order to give a momentum based representation of a soliton – anti soliton pair. We actually started with equation 11 and took a discrete Fourier transform presentation of a soliton – anti soliton pair in order to write:

$$[\phi - \phi_{classical}]_{initial,final} \approx \left[\frac{1}{L} \cdot \sum_n e^{-ik_n \cdot x_i} \phi(k_n) \right]$$

where L is the distance between a S-S', and $\phi(k_n)$ = Fourier representation of a S-S' pair in k_n space. As mentioned beforehand, we used what is known as a thin wall approximation to the S-S' pair which happens to be a square pulse of height $2 \cdot \pi$ and width L . Furthermore, we also managed to take a redo of the Bardeen presentation of a tunneling Hamiltonian as given by Tekeman [20] :

$$T_{mn} \equiv -\frac{\hbar^2}{2\mu} \int [\psi_0^* \nabla \psi_{mn} - \psi_{mn} \nabla \psi_0^*] \cdot dS \quad (16)$$

which in functional formulation we re wrote as:

$$(T_{IF})_{functional} \Big|_{\Psi_{(real)}} = \frac{-c_1}{2\mu} \int \left(\Psi_{initial}^* \frac{\delta \Psi_{final}}{\delta \phi(x)} - \Psi_{final} \frac{\delta \Psi_{initial}^*}{\delta \phi(x)} \right) \delta(\phi(x) - \phi_0(x)) \otimes \phi(x)$$

This has some similarity to a formulation written by David Soper in a write up of how he uses a Lagrangian density to form a current [26] as part of a derivation of Noether's theorem . We then proceeded to a 2nd variational derivative formulation of equation 19 which we recast into:

$$J \propto \frac{c_2}{2\mu} \int \left(\Psi_{initial}^* \frac{\delta^2 \Psi_{final}}{\delta \phi(x)_2} - \Psi_{final} \frac{\delta^2 \Psi_{initial}^*}{\delta \phi(x)_2} \right) \mathcal{G}(\phi(x) - \phi_0(x)) \delta \phi(x) \quad (17)$$

Once we have current in this sort of representation we are ready to address how to get conductivity behavior at the threshold which no longer has the singularity which made equation 15 so non physical. We should take note though that in transforming equation 18 to an overall current we can evaluate that we are actually starting off with wave functionals for equation 17 which are akin to what was done by Froreani et al with quasi Gaussian wave functionals similar to Fock vacuum spaces[21] . We should also note that the 2nd functional derivative notation used in equation 20 is akin to what was done by Boyanovsky et al [25] and helps us to eliminate cross terms in the current expression above, once we transform into k (momentum space). This allows us to avoid totally non physical conductivity behavior for conductivity at a threshold applied electric field value as equation 15 gives us without appealing to non physical potentials as has been done in prior publications [24] . Therefore we can say that when CDW scatters off impurities in the quasi one dimensional metallic lattice that we will see $(\sigma_{DC})_d \xrightarrow{E \rightarrow E_T} finite \ value$ and we will use this observation as part of what we will refer to as a quantum model due to the appearance of soliton-antisoliton pairs appearing when the applied electric field $E \geq E_T$. The soliton-antisoliton pairs will form a current, and this will occur when we have condensed electrons tunneling through a pinning gap at the Fermi surface in order to accelerate the CDW with an electric field.

Figure 5 captures the essence of this current behavior. We do not have a AC

[insert figure 5 about here]

electric field graph for $(\sigma_{AC})_d$ when $\max|E_{AC}| > E_T$, mainly because we have only modeled a non zero current composed of soliton-antisoliton pairs when $E_{DC} \geq E_T$. Note that the Bloch bands are tilted by an applied electric field when we have $E_{DC} \geq E_T$ leading to a soliton-antisoliton pair as shown in Figure 6. The slope of the

[insert figure 6 about here]

tilted band structure is given by $e^* \cdot E$ and the separation between the soliton-antisoliton pair is given by:

$$L = \left(\frac{2 \cdot \Delta_s}{e^*} \right) \cdot \frac{1}{E} \quad (18)$$

So, that, then we have $L \propto E^{-1}$. If we consider a Zener diagram of CDW electrons with tunneling only happening when $e^* \cdot E \cdot L > \varepsilon_G$ where e^* is the effective charge of each condensed electron and ε_G being a pinning gap energy, we have that figure 6 permits us to write :

$$\frac{L}{x} \equiv \frac{L}{\bar{x}} \cong c_v \cdot \frac{E_T}{E} \quad (19)$$

Here, c_v is a proportionality factor included to accommodate the physics we obtain via a given spatial (for a CDW ‘chain’) harmonic approximation of

$$\bar{x} = \bar{x}_0 \cdot \cos(\omega \cdot t) \Leftrightarrow m_{e^-} \cdot a = -m_{e^-} \cdot \omega^2 \cdot \bar{x} = e^- \cdot E \Leftrightarrow \bar{x} = \frac{e^- \cdot E}{m_{e^-} \omega^2}$$

Realistically, we have that $L \gg \bar{x}$, where we assume that \bar{x} is an assumed reference point an observer picks to measure where a soliton-antisoliton pair is on an assumed ‘one dimensional’ chain of impurity sites. Then, in a procedure explained in

appendix A, we have that there exists a soliton-antisoliton current due to a field theoretic modification of a tunneling Hamiltonian, to get:

$$|T_{IF}| \approx (2 \cdot \pi)^3 \cdot (n1)^2 \cdot c_i \cdot \left(\cosh \left(2 \sqrt{\frac{x}{2L}} - \sqrt{\frac{L}{2x}} \right) \right) \cdot c_f \cdot e^{-\alpha \cdot L \cdot \left[2 - (n1)^2 \cdot \left(\frac{L1}{L} \right)^2 \cdot \left(1 - \frac{L}{2x} \right) \right]} \quad (20)$$

where the magnitude of $|T_{IF}|$ is directly proportional to a current formed of soliton-anti soliton pairs, which is further approximated to be

$$I \propto C_1 \cdot 2 \cdot \left[\cosh \left[\sqrt{\frac{2 \cdot E}{E_T \cdot c_V}} - \sqrt{\frac{E_T \cdot c_V}{E}} \right] \right] \cdot \exp \left(-\frac{E_T \cdot c_V}{E} \right) \quad (21)$$

where we have $I = \langle j \rangle_{\text{Soliton-anti Soliton}}$. So, using this model of soliton-antisoliton current we get:

$$\left| (\sigma_{DC})_d = \frac{dI}{dE} \Big|_{E=E_T} \right| < \infty \quad (22)$$

instead of the infinite value for conductivity the purely classical model for direct current conductivity gives us when the applied electric field is at a threshold value as seen in equation 15. Equation 21 is very important since the current so obtained is zero for electric field values $0 \leq E < E_T$ and does not have the forced cut off given by the Zener expression given below for $E < E_T$:

$$I \propto G_p \cdot (E - E_T) \cdot \exp \left(-\frac{E_T}{E} \right) \quad \text{if} \quad E > E_T \quad (23)$$

0

Otherwise

Equation 21 thereby avoids the absurd situation given by equation 23 in figure seven

[insert figure 7 about here]

where we have a negative value for current given by the top expression of equation 23 if we do not impose the zero value for current if $E < E_T$. Equation 21 thereby indicates that the thin wall approximation to a soliton-antisoliton pair fits observed known experimental conditions in a way equation 23 only gives us by a non physical assumption put in to match known experimental data.

V. Conclusions

We included our classical simulation to show that additional deviations from known experimental results occur than just the well known singularity in differential conductivity if we use the washboard potential for how phase evolves in CDW transport. Our quantum mechanical tunneling expression removes the absurd singularity classically obtained by differential conductivity as an applied electric field reaches a known threshold value. This is in tandem with reconstructing an applied current versus an applied electric field graph matching experimental data taken in charge density wave experiments with NbSe_3 taken in 1985. Our DC conductivity result is inherently quantum mechanical and is from a current expression which avoids having negative current values if the electric field is below a threshold value. We find that our derivation permits a rigorous derivation of what was previously a Zener current expression with an arbitrary cut off put in for electric fields below a given threshold value.

We also have shown that the classical washboard potential model performs adequately for an AC electric field simulation of both conductivity and dielectric response values when the maximum value of the electric field is below a critical

threshold value. As discussed in the first part of our article, our simulation blew up at the threshold value of an applied electric field which we showed is linked to the production of soliton- antisoliton pairs in the DC case. In both cases, DC and AC electric fields, the classical model proved problematic in the region $E = E_T$. We believe that our interpretation is leading to a different procedure for analyzing CDW dynamics which more closely matches known experimental conditions than the non-quantum models have in the past. Furthermore, this tunneling Hamiltonian approach for obtaining current should prove useful for other weakly coupled matter fields which show up frequently in many physical systems than just the one we have analyzed above.

Appendix: A

Tunneling Hamiltonian Calculation of Soliton-antiSoliton ‘Current’

The quantum decay of the false vacuum [12] has been of broad scientific interest for over two decades. Several approaches have been proposed to treat quantum tunneling. One approach [12] is to use functional integrals to compute the Euclidean action, or “bounce” in imaginary time. In condensed matter, this method has been employed [13] to describe nucleation of cigar-shaped regions of true vacuum, with soliton-like domain walls at the boundaries, in a charge density wave. Another technique, the Schwinger proper time method [14], has been used to calculate the rates of particle-antiparticle pair creation in an electric field [15].

The tunneling Hamiltonian [16,17] involves matrix elements for the transfer of particles between initial and final wave functions. Josephson [18] employed the tunneling Hamiltonian in his theory of phase-coherent tunneling of Cooper pairs through an insulating barrier. However, this method has not been developed thus far for quantum field theory. The potential utility of the tunneling Hamiltonian is especially apparent when one considers systems of many weakly coupled fields. For example, Hawking et al.[19] point out that a universe can be nucleated by a cosmological instanton that is much larger than the Planck scale, provided there are sufficiently many matter fields. Moreover, a number of experiments on charge density waves and other condensed matter systems suggest quantum decay of the false vacuum, accompanied by the nucleation of soliton domain walls, even when the total action is large. Let us now construct a tunneling Hamiltonian explicitly, and

show that the corresponding expression we derive via an action principle is , indeed, intellectually the direct result of least action which has its intellectual genesis in the decay of the false vacuum Sidney Coleman [12] presented in 1977. To do this, we shall start with a method which on the surface appears to have little in common with least action principles.

Bardeen in 1960 [16] put forward an innovative thought experiment where he analyzed how a net flux of particles could penetrate a potential barrier set between two metallic regions. Here, unlike what Josephson did, Bardeen restricted himself to a specific line of inquiry which we can formulate as follows. Mainly, how does one interpret the transition probability of an electron to penetrate a barrier from points x_a to x_b ? Bardeen in the end in his 1960 article managed to derive a ‘matrix of transition’ we shall call $T_{if} = -i \cdot J(x_1)$ where ‘a’ \approx metal to the left of position x_a , and that ‘b’ \approx metal to the right of position x_b where each of the wave functions should be interpreted in terms of ‘quasi-particle occupation numbers’

(I.): Beyond grid point x_b we have any electron in a state m smoothly drops to zero. Therefore implying that “ ψ_0 is a solution for a Schrodinger equation with energy W_0 if $x < x_b$ ” but that “there is a region to the right of x_b where it is not a good solution”.

(II.)”Similarly we assume that ψ_{mn} with energy W_{mn} is a good solution for a wave function for $x > x_a$, but not for the region to the left of x_a where the wave function for quasi-particle n drops to zero.”

(III): However, for regions inside the barrier, we have that “Both ψ_0 and ψ_{mm} are good solutions in the barrier region $x_a < x < x_b$ ”. Given all of this we can write, assuming W_0 is $\cong W_{mm}$.

Now, let us follow the notation of E. Tekman [20] who has a reasonable upgrade of Bardeens notation.

$$T_{mm} \equiv -\frac{\hbar^2}{2\mu} \int [\psi_0^* \nabla \psi_{mm} - \psi_{mm} \nabla \psi_0^*] \cdot dS \quad (1)$$

where any current taken outside the range of x_a to x_b set equal to zero. In this situation, we have that ψ_0 is modified in the ‘Transfer Hamiltonian’ notation to be the wave function for a left hand side left electrode which is specified to be an ‘infinite’ (large) distance from the wave function designating a right hand side electrode ψ_{mm} . Furthermore, the integration is changed, subsequently, to be over the ‘area’ of a tunneling barrier, S_0 which if we make a transformation based upon changing to a ‘functional basis’ leads to

$$(T_{IF})_{functional} \Big|_{\Psi_{(real)}} = \frac{-c_1}{2\mu} \int \left(\Psi_{initial}^* \frac{\delta \Psi_{final}}{\delta \phi(x)} - \Psi_{final} \frac{\delta \Psi_{initial}^*}{\delta \phi(x)} \right) \delta(\phi(x) - \phi_0(x)) \delta \phi(x) \quad (2)$$

Here, we are assuming that $dS \approx n \cdot dx$ where n is the ‘height’ of the barrier between the two ‘half’ regions. Also,

$$dx \rightarrow \frac{\delta x}{\delta \phi} \cdot \delta \phi(x) \quad (3)$$

and

$$\nabla \Psi_{i,f} \approx \frac{\partial}{\partial x} \Psi_{i,f} \rightarrow \left(\frac{\delta x}{\delta \phi} \right)^{-1} \frac{\delta \Psi_{i,f}}{\delta \phi} \Big|_{\phi=\phi_0} \quad (4)$$

where $\left(\frac{\delta x}{\delta \phi} \right)^{-1} \Big|_{\phi=\phi_0} \cdot \frac{\delta x}{\delta \phi} \equiv \frac{\delta \phi_0}{\delta \phi} \approx \delta(\phi - \phi_0)$ leads to , after $\psi_0 \rightarrow \Psi_{initial}$ and

$\psi_{nn} \rightarrow \Psi_{final}$ are put into equation (1) , equation (2) above $\phi(x)$ may be chosen in whatever base we find convenient for this problem. In our applications, we used a D.F.T. (discrete fourier transform) which changes the value of equations (1) and (2) above. We will briefly allude to this later. But, we should for now discuss how we can modify these two equations via use of variational calculus .

What we should take into consideration is that one should try to set up the initial and final wave functions $\Psi_{initial}$ and/or Ψ_{final} as equal to $c_i \cdot \exp\left(-\beta \int L_i d\tau\right)$ and/ or $c_f \cdot \exp\left(-\beta \int L_f d\tau\right)$. In our condensed matter applications, we followed a convention which paralleled using a Gaussian functionals with ‘specific covariance’ Ω leading to wave functions very close to a ‘Fock Vacuum [21]

$$\Psi_{initial,final} \leftrightarrow |\Omega\rangle_{initial,final} \leftrightarrow \det^{1/4} \left[\frac{\Omega_R}{\pi} \right] \cdot \exp\left(-\frac{1}{2} \int \phi \cdot \Omega \cdot \phi\right)_{initial,final} \quad (5)$$

This is elaborated ,later. But, the idea is to define a space of functionals of a scalar field $\phi(x)$ and to define wave functionals for which we have an inner product space with $\langle \Psi_{initial} | \Psi_{final} \rangle = \int \delta \phi \Psi_{initial}^*(\phi) \Psi_{final}(\phi)$, where one has complex valued functionals with $|\Psi\rangle \leftrightarrow \Psi(\phi)$ and $\langle \Psi| \leftrightarrow \Psi^*(\phi)$. In a generic sense, we identify these wave functionals mentioned above with a least action formulation which is

shown below. One can look at either $\frac{\delta \Psi_{initial}}{\delta \phi(x)}$, or $\frac{\delta \Psi_{final}}{\delta \phi(x)}$, which is actually saying

that we have to look at $\left. \frac{\delta}{\delta \phi(x)} \left(\int L_{i,f} d\tau \right) \right|_{x='origin'}$ $\equiv 0$. It is useful to note that this is the

beginning of how people derive Noethers theorem in Classical and Quantum Field theory. Meaning in this situation one has that the net ‘current’ vanishes at the ‘origin’ (or at least is minimized at the origin!). Physically, one can interpret this, as we did in the case of soliton anti soliton pairs tunneling through a pinning gap, as indicating an ‘approximation’ in which one has a net cancellation of ‘positive direction’ and ‘negative direction’ current values at the ‘origin’. Presumably, away from the ‘origin’, we can assume $T_{if} = -i \cdot J(x) \neq 0$.

For explicit calculations of the current, J, let us now start with looking at, then, what happens when we look at:

$$\frac{\delta}{\delta \phi(x)} \left(\Psi_{initial} \Psi_{final} \right) \Big|_{\phi=\phi_0} = \left[\Psi_i \frac{\delta \Psi_f}{\delta \phi(x)} + \Psi_f \frac{\delta \Psi_i}{\delta \phi(x)} \right] \Big|_{\phi=\phi_0} = 0 \quad (6)$$

leading to, then $\Psi_i \frac{\delta \Psi_f}{\delta \phi(x)} \Big|_{\phi=\phi_0} \equiv -\Psi_f \frac{\delta \Psi_i}{\delta \phi(x)} \Big|_{\phi=\phi_0}$ which then will lead to a ‘current’ of

the form

$$(T_{IF})_{functional} \Big|_{\Psi(real)} \approx \frac{c_1}{2\mu} \int \left(\Psi_{final} \frac{\delta \Psi_{initial}}{\delta \phi(x)} \Big|_{\phi=\phi_0} \right) \delta(\phi(x) - \phi_0(x)) \delta \phi(x) \xrightarrow{x \rightarrow 'origin'} 0 \quad (7)$$

Equation six means that as we evaluate a net ‘current’ at the ‘origin’, we are minimizing this current as it approaches the mid point of a ‘sample space’ of objects measured .Conversely, having a non zero value for this ‘current’ when we set x not equal to this ‘origin value’ reinforces a multipole expansion interpretation of our problem, which we find conceptually elegant and useful.

As an actual application which started this research, we can observe soliton-anti soliton pairs tunneling through a ‘pinning gap’ of a ‘chain’ of a quasi one dimensional metal. In looking at this problem, we will write the wave functions as a one dimensional discrete Fourier transform by setting ,here, that (as mentioned above)

$$\Psi_{initial,final} = c_{initial,final} \cdot \exp(-\alpha \cdot \int dx [\phi - \phi_{classical}]_{initial,final}^2)$$

so

$$[\phi - \phi_{classical}]_{initial,final} \approx \left[\frac{1}{L} \cdot \sum_n e^{-ik_n \cdot x_i} \phi(k_n) \right] \quad (8)$$

where L is the distance between a S-S’, and $\phi(k_n)$ = Fourier representation of a S-S’ pair in k_n space. In this model situation, we used what is known as a thin wall approximation to the S-S’ pair which happens to be a square pulse of height $2 \cdot \pi$ and width L . We centered this pulse as being from $+ L/2$ to $- L/2$ spatially in order to take advantage of symmetry arguments which greatly simplified calculation of T_{IF} which will be shown later in this manuscript. We set that

$$\phi(k_n) = \sqrt{\frac{2}{\pi}} \cdot \frac{\sin(k_n L/2)}{k_n} \quad (9)$$

where k_n has dimensions equal to 1/length. So, equation (8) is dimensionless. Which is exactly what we want here. Furthermore, $\alpha \approx \left(\frac{1}{L}\right)$ so we can set $\alpha \int dx [\phi - \phi_{classical}]_{initial,final}^2$ as a dimensionless quantity, which we also need here. Furthermore, this integral above will be evaluated as a DFT. Before we do, let us say more about the situation represented by the integrand above in the initial and final states of a S - S' pair. Here, L_1 varies between L_0 (=minimal distance permitted between S - S') and L . Furthermore, $n \in (0,1]$. This being the case, we have that :

$$\Psi_{initial} = c_i \exp\left(-\left(\frac{\alpha}{L}\right) \cdot (2 \cdot \pi)^2 \cdot \sum_n |\phi(k_n)|^2\right) \quad (10)$$

In addition, we have

$$\Psi_{final} = c_f \exp\left(-\left(\frac{\alpha}{L}\right) \cdot (2 \cdot \pi)^2 \cdot \sum_n (1 - (n1)^2) \left(\frac{\sin\left(k_n L_1 / 2\right)}{\sin\left(k_n L / 2\right)}\right)^2 \cdot |\phi(k_n)|^2\right), \quad (11)$$

We obtained a T_{IF} expression for a pinning gap problem of (when $x \gg L$):

$$|T_{IF}| \approx (2 \cdot \pi)^3 \cdot (n1)^2 \cdot c_i \cdot \left(\cosh\left(2\sqrt{\frac{x}{2L}} - \sqrt{\frac{L}{2x}}\right) \right) \cdot c_f \cdot e^{-\alpha L \left[2 - (n1)^2 \left(\frac{L_1}{L}\right)^2 \left(1 - \frac{L}{2x}\right) \right]} \quad (12)$$

where we are explicitly using that we have set :

$$E_0 \approx (E_0)_{init} (2 - (n1)^2 (L_1/L)^2 (1 - \frac{L}{2x} + i \cdot \left(1 + \frac{L}{2x}\right))) \quad (13)$$

where

$$\alpha \cdot L \approx \frac{(E_0)_{init}}{E} \quad (14)$$

Here, n_1 is between zero and one, and represents how a soliton – anti soliton pair evolves in height over a period of time. Furthermore, L_1 is how the soliton and the anti soliton vary in distance from each other. We can argue here that we actually have a linkage to a Langrangian based ‘least action’ argument due to equations 12,13, and 14 as well as $(c_2) \cdot \exp\left(\frac{-E_o}{E}\right)$ being equivalent with the ‘False vacuum’ formulation

of the ‘decay rates’ of both Coleman and Maki [17,22] . Making this final linkage, however, requires that we make explicit how we can connect

$$\Psi_{i,f} = c_{i,f} \cdot \exp(-\alpha \cdot \int dx [\phi - \phi_{classical}]_{i,f}^2) \text{ and } c_{i,f} \cdot \exp\left(-\beta \int L_{i,f} d\tau\right). \text{ To start}$$

this, note that if $L_{i,f} \equiv \frac{m_{eff}}{2} \int \left[\frac{dx}{d\tau}\right]^2 dx$ and that $\left[\frac{dx}{d\tau}\right] \approx v \equiv \text{constant velocity}$, and

that $\phi - \phi_{classical} \equiv \Delta x \cdot \frac{d}{dx}(\phi_{classical})$, then one can inter exchange the dx and $d\tau$

integration order in $\int L_{i,f} d\tau$. Doing so permits us to write

$$\beta \int L_{i,f} d\tau = \beta \cdot \frac{m_{eff} \tau}{2} \int v^2 \cdot dx \approx \beta \cdot \frac{m_{eff} \tau}{2} \cdot v^2 \int dx \equiv \alpha \cdot \int \left(\Delta x \cdot \frac{d}{dx} \phi_{classical}\right)^2 dx \text{ which}$$

$$\text{then leads to } \left(\Delta x \cdot \frac{d}{dx} \phi_{classical}\right)^2 \equiv \frac{\beta}{\alpha} \cdot v^2 \frac{m_{eff} \tau}{2} \Rightarrow \phi_{classical} \approx \sqrt{\frac{\beta}{\alpha} \cdot v^2 \cdot \frac{m_{eff} \tau}{2 \cdot (\Delta x)^2}} \approx 2 \cdot \pi$$

when we are in the region where a $S - S'$ pair is, and zero otherwise. Usually, $v \approx 10^{-3} c$, where c is the speed of light. This will necessitate very short transition times.

We are restricting ourselves to ultra fast transitions of CDW which is realistic and which reflects the fact that the CDW moves very infrequently, with sudden

abrupt transitions. However, our method for forming this matrix of transition is much more general than this and it should be understood that whatever $|T_{IF}|$ is derived is heavily dependent upon the dimensionality of the ‘basis’ chosen to evaluate our ‘current’ expression.

How we construct $|T_{IF}|$ is a far-reaching problem, which could impact many areas of physics. For example, topological defects, such as flux vortices, play an important role in the cuprates and other type-II superconductors. Magnetic relaxation rates that depend weakly on temperature up to 20 K [23], or even decrease with temperature, suggest that Abrikosov vortices may tunnel over a wide temperature range. Moreover, the consistently low $I_c R_n$ products of cuprate Josephson devices suggest that Josephson vortex-antivortex pair creation may occur when the current is much smaller than the “classical” critical current $I_0 \sim \Delta/R_N e$. In cosmology, the existence of many matter fields may facilitate quantum nucleation of a universe even when the total action is large, as suggested by Hawking et al [19]. Finally, the extraordinary rapidity of first-order phase transitions, such as the palpably visible nucleation of ice in supercooled water, suggest a possible similarity to the decay of the false vacuum.

Figure captions

FIG 1 Average phase $\langle \phi \rangle$ plotted against time (for E_{dc}) with $\langle \phi \rangle$ stabilizing if $E_{dc} < E_{th}$ and $\langle \phi \rangle$ monotonically increasing if $E_{dc} > E_{th}$.

FIG 2 This is conductivity in the case when one has only an electric field E_{dc} with a magnitude less than E_{th}

FIG 3 Comparison of scaled dielectric values when one has signal frequency $\omega \leq \omega_c$ i.e. near a critical value ω_c .

FIG 4 This, above, is a direct comparison of plots, which does highlights the divergence from linearity occurring as frequency drops. The dielectric is infinite valued when $E=E_{th}$

FIG 5 The above figures represents the formation of soliton-anti soliton pairs along a 'chain'. The evolution of phase is spatially given by $\phi(x) = \pi [\tanh b(x-x_a) + \tanh b(x_b - x)]$

FIG 6 This is a representation of 'Zener' tunneling through pinning gap with band structure tilted by applied E field.

FIG 7 Experimental and theoretical predictions of current values

+

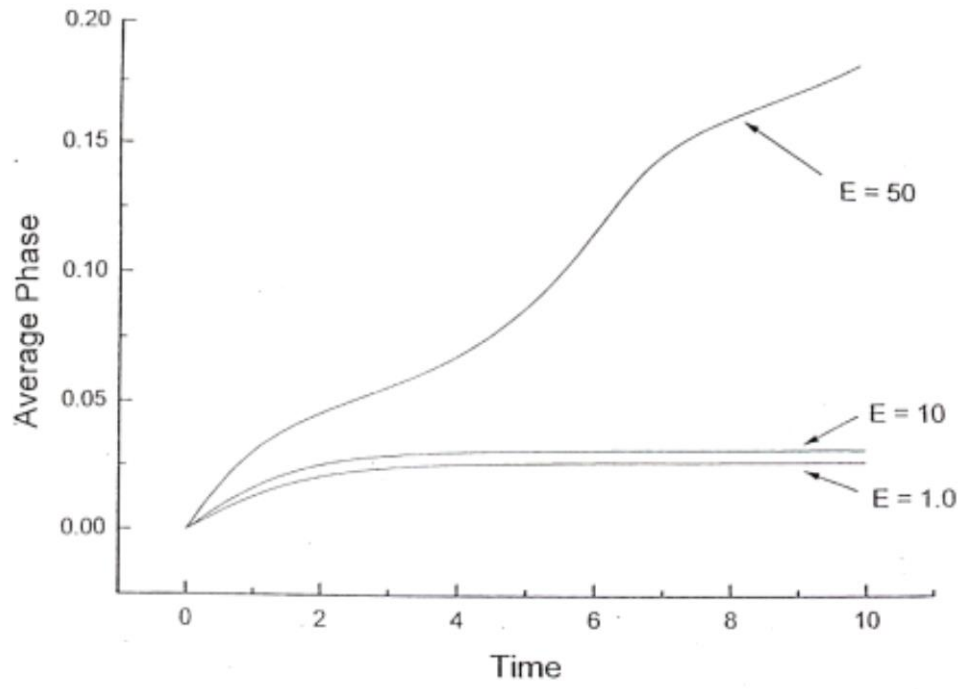


Figure 1

Beckwith et al

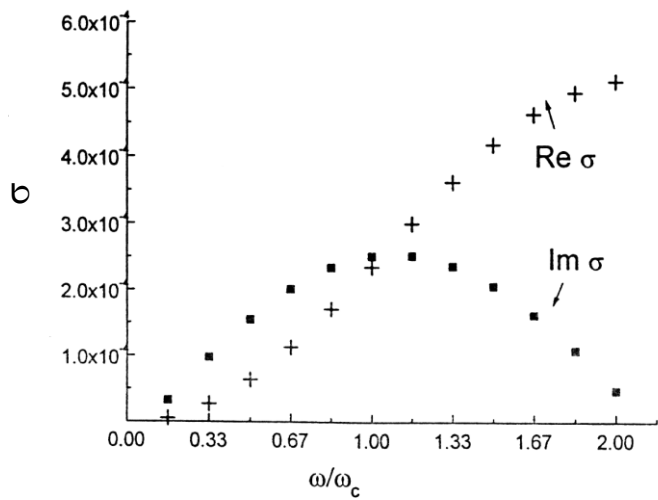


Figure 2

Beckwith et al

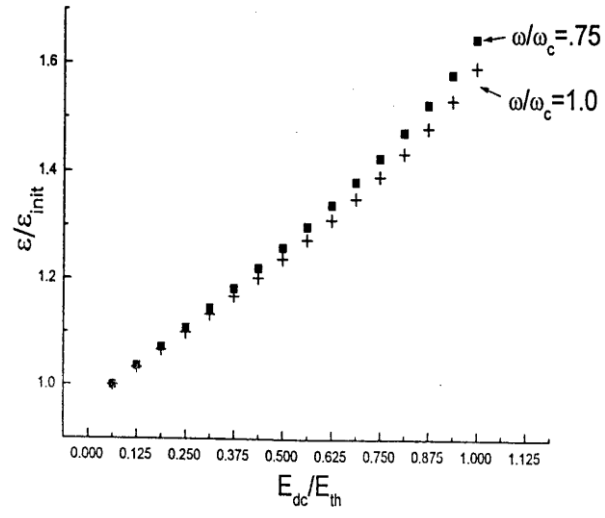


Figure 3

Beckwith et al

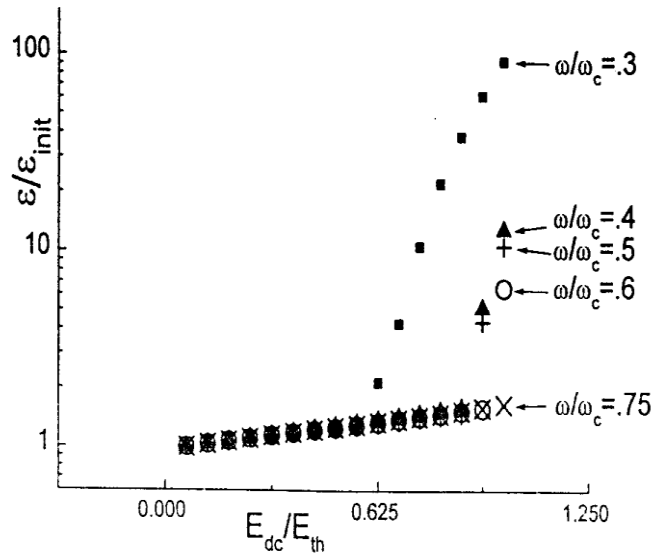


Figure 4

Beckwith et al

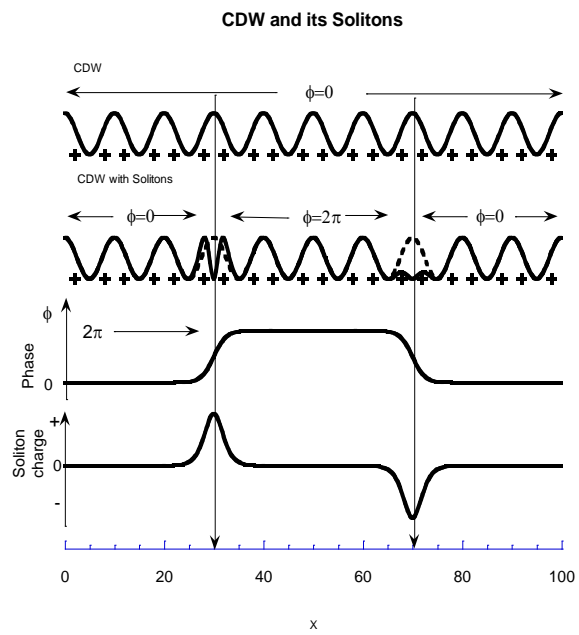


Figure 5

Beckwith et al

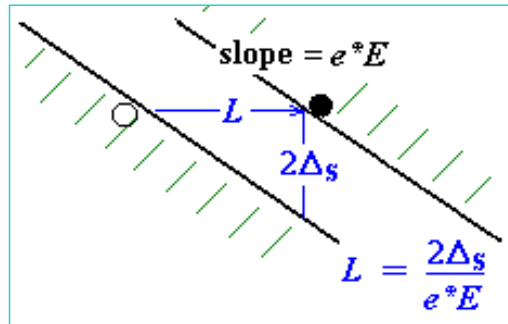


Figure 6

Beckwith et. al

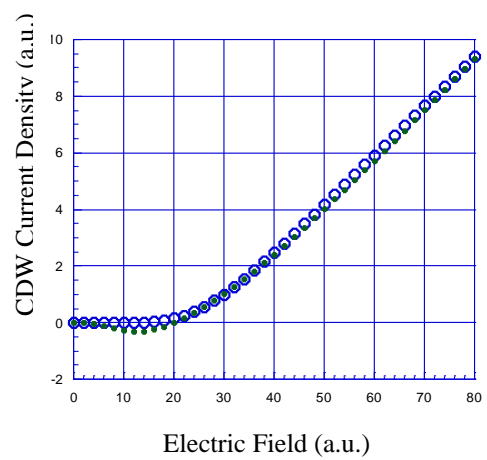


Figure 7

Beckwith, et. al

REFERENCES

- 1: P.B Littlewood ; *Phys.Rev B* **33**, 6694 (1986)
- 2: H. Fukuyama and P.A Lee ; *Phys.Rev. B* **17**,535 (1977)
- 3: P.A.Lee and T.M. Rice ; *Phys.Rev. B* **19**,3970(1977)
- 4: S. Kagoshima, H.Nagasawa and T.sambongi ; ‘One Dimensional Conductors’ , Springer –Verlag,1977 . See equation 2.74
- 5: J.H. Miller,J. Richards,R.E. Thorne,W.G.Lyons and J.R. Tucker ; *Phys.Rev. Lett.* **55**,1006 (1985)
- 6: P.B Littlewood ; *Phys.Rev B* **33**, 6694 (1986) . See equation 2.5
- 7: P.B Littlewood ; *Phys.Rev B* **33**, 6694 (1986). See equation 2.6
- 8: N. Teranishi and R. Kubo ; *J.Physics.Soc.Jpn.* **47**,720 (1979)
- 9: L. Pietronero and S.Strassler ; *Phys.Rev. B* **28**,5863 (1983) ; H. Matsukawa and H. Takayama ; *Solid State Commun.* **50**,283(1984)
- 10: Private communications with Bill Mayes II, U. of Houston Phys. Dept.
- 11: G. Gruner ; ‘ Density Waves in Solids’, Addison Wesley, 1994, See Figure 10.1 and Formulae 10.2
- 12: S. Coleman ; *Phys.Rev.D* **15**, 2929 (1977)
- 13: I.V. Krive and A.S. Rozhavskii ; *Soviet Physics JETP* **69**,552 (1989)
- 14: J. Schwinger ; *Phys.Rev.***82**, 664 (1951)
- 15: Y. Kluger, J.M. Eisenberg , B. Sventitsky, F. Cooper and E. Mottola ; *Phys.Rev.Lett.* **67**,2427 (1991)
- 16: J. Bardeen ; *Phys.Rev. Lett.* **6**, 57 (1961)
- 17: M. H. Cohen,L.M. Falicov and J.C. Phillips ; *Phys.Rev.Lett.* **8**, 316 (1962)

- 18: B.D. Josephson ; *Phys.Lett.* **1** ,251 (1962)
- 19: S.W. Hawking , T. Hertog and H.S. Reall ; *Phys.Rev.* **D 63**, 083504 (2001)
- 20: E. Tekman ; *Phys.Rev.* **B 46**, 4938 (1992)
- 21: R. Floreeani and R.Jackiw, *Phys.Rev.* **D 37**, 2206 (1988)
- 22: K. Maki ; *Phys.Rev.Lett.* **39**, 46 (1977)
- 23: Y.Y. Xue , Z.J.Huang, P.H.Hor and C.W. Chu , *Phys.Rev.* **B 43** , 13598 (1991)
- 24: D. S. Fisher, *Phys.Rev.* **B 31**, 1396 (1985)
- 25: D. Boyanovsky, F. Cooper , H. de Vega, and P. Solano , *Phys.Rev.* **D 58** ,25007 (1998)
- 26: Davison Soper, ‘Classical Field theory’ , Wiley, 1976, pp 101-108. In particular, equation 9.13 of page 101